JOURNAL OF VIROLOGY, Sept. 1993, p. 5126–5138
0022-538X/93/095126-13$02.00/0

Vol. 67, No. 9

Protein Species of the Parvovirus Minute Virus of Mice Strain MVMp: Involvement of Phosphorylated VP-2 Subtypes in Viral Morphogenesis

JUAN F. SANTARÉN,[1] JUAN C. RAMÍREZ,[1,2] AND JOSE M. ALMENDRAL[1,2]*

Centro de Biología Molecular "Severo Ochoa" (UAM-CSIC), Universidad Autónoma, Cantoblanco, 28049 Madrid,[1] and CIEMAT, Avenida Complutense 22, 28040 Madrid,[2] Spain

Received 31 March 1993/Accepted 19 May 1993

The pattern of induced protein species of the prototype strain of the parvovirus minute virus of mice was determined in permissive A9 mouse fibroblast cells by high-resolution two-dimensional gel electrophoresis. Identities of the viral proteins in the gels were assigned by probing two-dimensional blots with antisera raised against either purified capsids (recognizing VP-1 and VP-2) or specific coding regions of the nonstructural proteins (NS-1 and NS-2) expressed as β-galactosidase fusion products in bacteria. All viral proteins showed posttranslational modifications, phosphate being a common substituent. The NS-1 protein migrated as a basic polypeptide in the pI range of 7.4 to 7.8 with multiple stages of modification and as a likely minor but hyperphosphorylated component in the neutral region of the gel. The NS-2 isoforms were resolved at a pI value close to 5.5 as three groups of unevenly phosphorylated polypeptides, each composed of at least two protein species. Both VP-1 and VP-2 structural polypeptides were induced as heterogeneous phosphoproteins. The major VP-2 protein could be resolved in the form of a consistent pattern of three abundant (a to c), two intermediate (d and e), and one meager (f) neutral isoelectric focusing species or subtypes. This posttranslational modification precedes and is uncoupled from viral assembly, and all of the VP-2 subtypes are packaged into empty capsids at the induced stoichiometry. However, intracellular full virions harbored additional phosphorylated subtypes (g to l) and a subtle rearrangement in the whole VP-2 composition, while mature virions purified from lysed cultures lacked these subtypes, coordinately with the emergence of six neutral VP-3 subtypes. Thus, the virion coat undergoes a chemical transition entailed by genome encapsidation, in which phosphates seem to play a major role, triggering the preferential proteolytic cleavage of the more acidic VP-2 subtypes to VP-3. Parvoviruses, with small coding capacity, may regulate some morphogenetic steps, such as assembly, genome encapsidation, and maturation, by posttranslational modifications of their structural proteins.

Minute virus of mice (MVM) belongs to the genus *Parvovirus* of the family *Parvoviridae* (70), a group of small autonomously replicating viruses with a nonenveloped 20-nm icosahedral capsid (reviewed in reference 16). The MVM genome is a linear single-stranded DNA 5,149 bases in length (3), folded at both termini in self-complementary hairpin structures (4, 59), and organized as two transcriptional units (57) that code for the nonstructural (NS) and structural (VP) polypeptides, respectively. Despite their genetic simplicity, parvoviruses have evolutionally combined the alternative splicing, proteolytic processing, and multifunction of gene products as molecular strategies that enhance their coding capacity.

The MVM R1 genomic transcript expressed from the P4 promoter is translated into the 85-kDa nonstructural NS-1 protein (13). This phosphorylated cytotoxic nuclear protein (9, 14, 52) contains ATPase and helicase activities (84), and it has multiple functions in the virus life cycle, such as DNA replication and packaging of progeny single-stranded DNA (ssDNA) (17, 19, 61) and transcription regulation from viral promoters (21, 22, 60). NS-1 is covalently linked to the 5′ end of newly synthesized DNA and is packaged outside the virus particle in most virions released from A9 cells (17). This linkage may be cleaved without impairment of virus infectivity, a process that is mediated by extracellular nucleases or upon subsequent entry into cells. Splicing of the large intron of the virus genome yields the R2 mRNA coding for the 25-kDa NS-2 protein, which shares a common N-terminal domain of 85 amino acids with NS-1 (15). Two alternate splicings between map units 44 to 46 excise the small intron common to all transcripts and result in three NS-2 protein isoforms which differ at their carboxyl termini (32). Each NS-2 isoform has its phosphorylated counterpart and shows characteristic subcellular compartmentalization and stability (18). The NS-2 proteins are required for viral replication and infectious virus production (40, 45), which may be the consequences of a primary effect exerted at the level of translation of viral mRNA (46).

The same two splicings affect the R3 messengers generated from the promoter at map unit 38 (35). The result is that the two capsid polypeptides VP-1 (83 kDa) and VP-2 (64 kDa), which are the primary translated products (16), have distinct initiation codons, but because they are coded in the same reading frame, these proteins are different in size but have identical amino acid sequences (8, 78). In infected cells and viral particles, the ratio between VP-1 and VP-2 is determined by the frequency at which these two alternate splicings are used (10, 32, 35, 43). MVM grown in culture contains a large quantity of noninfectious empty capsids with a buoyant density of 1.32 g/ml, composed exclusively of VP-1 and VP-2 proteins (74). Full particles with encapsidated viral DNA are resolved in CsCl gradients as two populations of densities of 1.47 and 1.42 g/ml that contain

* Corresponding author.

variable amounts of a third structural polypeptide, VP-3, derived from cleavage of the N-terminal domain of VP-2 once the particle is assembled (77). VP-3 may be absent in preparations performed by other methods (23); in fact, particles are equally infectious regardless of their density or VP-2/VP-3 protein content (50). The ratio of viral protein VP-2 to VP-3 depends on the host cell and the postinfection time; at early times VP-2 is predominant, but late in the infection VP-3 is the major form (77). VP-2-to-VP-3 conversion accompanies the infection process of internalized virus in a time-dependent manner (50). In vitro, cleavage of VP-2 to VP-3 may be partially mimicked by digestion of full particles with trypsin and to a lesser extent by chymotrypsin (53, 78). However, VP-1 was always resistant to proteolytic cleavage, as was VP-2 in empty capsids.

The difference in accessibility to proteases of VP-2 in full and empty particles led to the proposal that viral DNA encapsidation must alter capsid structure to expose the VP-2 processing site (16), and although the nature of this alteration has remained elusive, ultrastructure data have supported this notion. Crystallographic studies provided a three-dimensional atomic structure of the canine parvovirus icosahedron (80). The virion is composed of 60 asymmetric subunits (predominantly VP-2, also VP-3, and some VP-1) in an eight-stranded antiparallel β-barrel topology, each fitting a loop of 11 nucleotides of the ssDNA stabilized by a metal ion. Part of the amino terminus of VP-2 projects outward in full but not empty virions, in agreement with the aforementioned protease sensitivity of VP-2 in the full virions. Likewise, two types of biochemical data agree with the lack of sensitivity to proteases of the VP-1 N terminus. First, chemical cross-linking experiments revealed VP-1 clustering in empty capsids (51), whereas in the full virions, the protein was not accessible to the chemicals. Second, aggregates of more than one VP-1 molecule bind to the 3′ hairpin of the viral genome in full virions (83), an interaction that occurs internally in the particles, probably mediated by the unique basic N-terminal region of VP-1 (77). Therefore, VP-1 and VP-2 show asymmetric topology in the virus particles, which may indicate different functions for these proteins in maturation and viral infection; this matter deserves further investigations. In this regard, it was recently demonstrated that VP-2 is necessary for encapsidation of viral genome, while VP-1 seems to play a role in the virus progeny infectivity (81).

Parvovirus multiplication requires functions expressed transiently during the S phase (69) of target cells at specific differentiation stages (75). However, cells transformed by a variety of agents are less restricted with respect to parvovirus multiplication (44, 64), and this oncotropism was correlated with an increase in the transcription of viral genes (12) and in the activity of the viral early promoter (72). Viral determinants of cell permissiveness have been studied for canine parvovirus (54, 55, 82) and for two strains (p and i) of MVM. The tropism of these MVM strains has been characterized by the productive or restrictive infections in cell lines and primary cells in vitro (68, 76) and found to be determined by the interaction of intracellular factors (73) with a VP domain (2, 27) of the incoming particle (28). Several amino acid changes between MVM strain i and an extended-host-range variant were mapped within this capsid determinant (5), two of which conferred coordinately the greatest infectivity for fibroblasts (6).

A precise understanding of the interactions between cellular and viral factors at the molecular level is required in order to address current questions of parvoviruses biology, such as why some but not all proliferating normal, transformed cells and tissues are permissive to virus infection, or to define discrete steps of the infection process such as internalization, uncoating, and viral packaging. For this purpose, a comprehensive study of the viral protein modifications that occur during the viral life cycle is needed. A two-dimensional (2-D) analysis of the microheterogeneity and phosphorylation stage of the MVM structural proteins was performed several years ago (56). In this report, we have reexamined that work and extended it to include the NS proteins in order to provide a detailed two-dimensional (2-D) map of the MVM prototype strain (MVMp)-induced proteins and their phosphorylation stages in permissive A9 cells. Moreover, working under conditions that allow good resolution of individual VP-2 protein species, we were able to demonstrate the distinct modifications that assembly, genome encapsidation, and virus maturation impose on the major capsid protein. These data have led us to propose an integrative model of coat protein phosphorylations in MVMp morphogenesis.

MATERIALS AND METHODS

Cells. The A9 mouse fibroblast and NB324K simian virus 40-transformed human newborn kidney cell lines, described as hosts for MVMp (76), were maintained in Dulbecco modified Eagle medium (DMEM) supplemented with 5% heat-inactivated fetal calf serum (FCS). The origin of our cell lines has been reported elsewhere (68). NIH 3T3, a cell line nonpermissive for MVM infection (44, 64), was obtained from R. Bravo (Princeton, N.J.) and cultured similarly.

Purification of labeled MVMp particles. The prototype parvovirus MVMp, originally isolated from a murine adenovirus stock (20) and generously provided by Jean Rommelaere (Heidelberg, Germany), was grown and plaque assayed in the A9 cell line essentially as described previously (77). Virus stocks were prepared from infections at low multiplicity and purification by density gradients as described before (68) and stored at −80°C. All infections described in this report were performed with purified virus at a multiplicity of infection of 5 to 10 PFU per cell.

^{35}S- and ^{32}P-labeled capsids and virions for 2-D analysis were similarly purified. Plates to be used for the analysis of mature virus that harbors the VP-3 polypeptide were harvested when they exhibited a generalized cytopathic effect (at 60 h postinfection [hpi]) by direct scraping of the cells into medium in the presence of protease inhibitors (1 mM phenylmethylsulfonyl fluoride [PMSF] and 5 mM NaF), and sodium dodecyl sulfate (SDS) was added to 1%. For the analysis of immature full virions, cell monolayers were washed three times with phosphate-buffered saline (PBS) at 16 hpi and scraped in 20 mM Tris (pH 8.5)–1 mM EDTA–1 mM PMSF–5 mM NaF–1% SDS; DNA was sheared by flushing through a 25-gauge needle. The respective homogenates were centrifuged for 18 h at 16,000 rpm and 15°C in a Beckman SW40 rotor (30,000 × *g*) through 2 volumes of a 20% sucrose cushion in 50 mM Tris (pH 8.0)–0.1 M NaCl–1 mM EDTA–0.2% SDS. The virus pellets were resuspended in 0.5 ml of 50 mM Tris-HCl (pH 7.5)–5 mM $MgCl_2$–5 mM $CaCl_2$–10 mM NaCl–0.1 mM PMSF–5 mM NaF; clumps were disaggregated by gentle sonication and digested with DNase I (25 μg/ml; Worthington), RNase A (20 μg/ml), and RNase T_1 (20 U/ml; Boehringer Mannheim) for 30 min at 37°C. The suspensions were brought to 10 ml of 20 mM Tris (pH 8.5)–1 mM EDTA–0.2% Sarcosyl, adjusted to a density of 1.38 g/ml in CsCl by refractometry, and centrifuged to

equilibrium for 42 h at 48,000 rpm and 5°C in a Beckman Ty65 rotor (150,000 × *g*). Gradients were fractionated, and label distribution was determined by scintillation counting. Empty capsids and virions were then rebanded separately twice more by centrifugation to equilibrium in CsCl gradients adjusted to densities of 1.32 and 1.42 g/ml, respectively. In these preparations, counts at a density of 1.47 g/ml corresponding to heavy full particles (50, 78) were insufficient to be analyzed by 2-D gels.

Radiolabeling of cells and viruses. The following procedure was used for high-specific-radioactivity labeling in the analysis of total induced proteins. Adherent A9 cells were seeded at a density of 25,000 cells per cm^2 in 24-well plates and cultured overnight in DMEM supplemented with 10% FCS. Once infected or mock infected, cells were labeled at 12 to 16 hpi in 300 μl of either methionine-free DMEM–10% dialyzed FCS–300 μCi of [^{35}S]methionine (Amersham SJ5050) or phosphate-free DMEM–10% dialyzed FCS–300 μCi of [^{32}P]phosphate (carrier free; Amersham PBS13) to visualize phosphoproteins. Cells were harvested at given times by washing the cells twice with PBS and scraping the monolayer in 100 μl of 2-D lysis buffer (47).

To obtain purified ^{35}S- and ^{32}P-labeled virions and capsids, 4×10^6 growing A9 cells in 90-mm-diameter dishes were infected and labeled according to two different protocols. Cells to be analyzed for immature virus purification were labeled at 12 to 16 hpi with either methionine-free medium containing 10% dialyzed FCS, and 200 μCi of [^{35}S]methionine per ml or phosphate-free medium containing 10% dialyzed FCS and 1 mCi of [^{32}P]phosphate per ml. For mature virus production, cells were labeled from 9 hpi in methionine-free medium supplemented with 10% normal medium, 5% dialyzed FCS, and 200 μCi of [^{35}S]methionine per ml or in phosphate-free medium containing 5% dialyzed FCS and 0.5 mCi of [^{32}P]phosphate per ml. At the times indicated above, the cells were processed for purification of virus by CsCl gradients.

2-D gel electrophoresis. 2-D gel electrophoresis was performed as described by O'Farrell (47, 49), with minor modifications (67). Briefly, the first-dimension separations for resolving neutral and acidic proteins were performed in 4% (wt/vol) polyacrylamide gels (230 by 2.3 mm) containing 2% ampholytes (1.6%, pH 5 to 7; 0.4%, pH 3.5 to 10) at 1,200 V for 20 h (isoelectric focusing [IEF]). Separations for resolving basic proteins were made on 4% (wt/vol) polyacrylamide gels (150 by 2.3 mm) containing 2% ampholytes (1% pH 7 to 9; 1% pH 8 to 9.5) at 400 V for 4.5 h (nonequilibrium-pH gel electrophoresis [NEPHGE]). The second-dimension separations were carried out in a 15% polyacrylamide gel (24 by 24 cm) run at room temperature overnight. Gels loaded with ^{35}S-labeled samples were processed for fluorography (37), and those from ^{32}P labeling were dried and exposed with an intensifying screen to X-ray film (Kodak X-Omat) at −80°C for various periods of time.

For high-resolution analysis, 10^6 trichloroacetic acid-precipitable cpm (approximately equivalent to 2,000 cells) were routinely applied per gel in samples of total proteins. Purified labeled capsids or virions were dialyzed against 10 mM Tris-HCl (pH 7.5)–0.5 mM EDTA, lyophilized, and incubated in 2-D lysis buffer at 37°C for 30 min. Usually 5×10^4 cpm of ^{35}S or 2×10^5 cpm of ^{32}P from these samples was applied per gel. In comparative analysis of protein forms, both first and second dimensions were run in parallel, and the films were matched for common spots. When required, spots in the autoradiograms were quantitated by laser scanning in a Molecular Dynamics 300A apparatus.

Expression in bacteria and purification of β-Gal–NS fusion proteins. Specific coding regions of the MVMp NS-1 and NS-2 proteins (15) were engineered at the C termini of the β-galactosidase (β-Gal) gene, using the pEX series of bacterial expression plasmids, which have a polylinker into the *lacZ* gene in all three translational reading frames (73). Plasmid pEX1-NS-1 was obtained by blunt-end ligation, at the *Sma*I site of pEX1, of the *Pvu*II-*Xho*I fragment that includes nucleotides 761 to 2070 of the MVMp genome (nucleotide numbering is as in reference 3), followed by fill-in with Klenow polymerase. This cloning procedure places the NS-1 coding region of this fragment (frame 3 of the major left-hand open reading frame of the MVM genome) and the β-Gal protein in the same frame. For NS-2 expression, plasmid pEX2-NS-2 was constructed similarly by cloning the *Xho*I-*Pvu*II fragment (nucleotides 2070 to 2850) at the *Sma*I site of pEX2 in the coding frame of the NS-2 second exon (frame 2 of the MVM genome). Ligation mixtures were transformed into *Escherichia coli* JM109, and recombinant plasmids were isolated. The fidelity of the constructs was checked by sequencing through the cloning sites, using the dideoxynucleotide chain termination method, with a 17-mer β-Gal oligonucleotide that primes 50 bases upstream from the pEX multicloning site. DNA manipulations were performed by conventional procedures (66).

The pEX vectors express large quantities of fusion proteins under the control of the p_R promoter of λ bacteriophage. Plasmids with in-frame constructions were transformed into *E. coli* pop2136 containing the *c*I *ts*857 repressor, and individual colonies were screened for the highest induction of the Cro–β-Gal–NS fusion proteins at 42°C as described previously (73). For immunizations, fusion proteins were purified by taking advantage of the large quantity of hybrid insoluble protein that in the form of inclusion bodies is produced by the pEX vectors. Inclusion bodies were prepared, washed in guanidine hydrochloride at low concentration (36), and run on preparative SDS-polyacrylamide gels. A small vertical strip was stained, the region of the gel corresponding to the fusion protein was excised, and the proteins were electroeluted into chambers as described previously (34), running at 24 V overnight in 100 mM glycine–20 mM Tris base–0.01% SDS. Protein recoveries were estimated by comparison with known amounts of pure β-galactosidase on SDS-polyacrylamide gels.

Antisera. Anti-NS polyclonal antisera were raised in 10-week-old BALB/c/C57BL female mice by intraperitoneal injections of each mouse with 50 μg of purified fusion protein emulsified in Freund's complete adjuvant the first time, followed by four boost injections with the same dose in incomplete adjuvant. Anesthetized animals were bled through the ocular orbital 7 days after the last dose. Serum raised against purified β-Gal from pEX1-transformed bacteria was used as a control.

A hyperimmune MVMp capsid antiserum was raised in rabbits by injections (100 μg per dose) of density gradient-purified empty capsids as follows: a first dose with capsids emulsified in Freund's complete adjuvant injected at multiple sites along the back, one subcutaneous and intramuscular boost in incomplete adjuvant, and two further intravenous and intramuscular doses in PBS. Bleeding was done 10 days after the last injection.

Immunoblot analysis. Commonly 10^6 infected A9 cells were scraped in 2-D lysis buffer at 16 hpi, mixed with 10^6 cpm of an equivalent sample ^{35}S-labeled to high specific activity (see above), and submitted to 2-D electrophoresis. Proteins resolved in 2-D gels were electrotransferred onto

nitrocellulose membranes (79) at 130 mA for 8 h. Filters were incubated for 4 h at room temperature with the corresponding antibody diluted in PBS containing 10% bovine serum. The filters were subsequently incubated with peroxidase conjugated anti-rabbit immunoglobulin G (Jackson ImmunoResearch Laboratories) for 2 h in the same buffer. After extensive washing with PBS containing 0.05% Tween 20 and equilibration of the membrane in a peroxidase buffer, the immunocomplexes were visualized by using 4-chloronaphthol (Merck) as a substrate (30). Filters were vacuum dried and exposed for autoradiography to precisely assign the signals in the films to the spots of the nitrocellulose-bound proteins.

RESULTS

2-D identification of the MVMp-induced proteins in A9 cells. Antibodies raised against denatured antigens usually have enhanced ability to immunoreact in blots. Thus, we chose to raise antibodies against β-Gal–NS fusion proteins purified from SDS-gels to increase the chance of detecting the NS proteins in 2-D blots. A pUC-derived plasmid containing the entire MVMp genome was constructed from viral intermediate replicative forms (to be described elsewhere), and specific coding sequences of the NS-1 and NS-2 proteins were inserted in the pEX vectors according to the cloning procedure outlined in Fig. 1. These vectors are designed to express the desired polypeptide fused to the carboxy end of Cro–β-Gal in the form of insoluble inclusion bodies, factors that should minimize the described degradation of bacterially expressed MVM–β-gal fusion products (15). Bacteria carrying the *c*I *ts*857 gene, when transformed by pEX vectors, produce upon induction at 42°C a fusion protein easily recognizable in gels by a molecular weight larger than those of most other proteins in the culture and the high level of expression that may account up to 25% of the total SDS-extracted cell protein (73). The cloning strategy predicts the synthesis of a 160-kDa Cro–β-gal–NS-1 fusion protein, resulting from the expression of 436 NS-1 amino acids that end with a β-Gal stop codon. The cloned NS-2 region codes for 70 amino acids and provides its own terminator codon; therefore, a 125-kDa Cro–β-Gal–NS-2 fusion protein would be expected. In agreement with these predictions, cultures of bacteria transformed with these plasmids yielded upon promoter induction large quantities of apparently intact proteins with approximately these expected sizes (not shown). The fusion proteins were purified by preparative gel electrophoresis and used to raise specific antibodies as described in Materials and Methods.

Asynchronously growing A9 cells infected by MVMp were harvested at 16 hpi and mixed with an equivalent ^{35}S-labeled sample, and the total lysate was subjected to 2-D electrophoresis and immunoblot analysis. Blots probed with antiserum raised against the purified β-Gal–NS-1 fusion protein identified NS-1 as a 80- to 85-kDa protein at the basic border of the IEF gels that could be efficiently recognized by our monospecific antibody only in overloaded blots (Fig. 2A). The polyclonal β-Gal–NS-2 antiserum demonstrated the three NS-2 protein isoforms at the acidic region of the IEF gels, in the form of three pair of spots with an apparent molecular size close to 25 kDa (Fig. 2B). The three isoforms were equally immunoreactive with the monospecific antiserum, although the carboxy-terminal domains of the P and L isoforms (according to the nomenclature proposed in reference 18) that are coded in different reading frames (32) would not be expressed in the β-Gal–NS-2 protein used as antigen (Fig. 1C). Structural MVMp proteins were recognized by the hyperimmune purified capsid antiserum at positions corresponding to the known molecular weights for these proteins (16, 77, 78). VP-1 (82 kDa) migrated in the basic NEPHGE gels (Fig. 2C), and the major structural protein VP-2 (64 kDa) migrated toward the neutral region of the IEF gels (Fig. 2D). We observed the microheterogeneity described for these proteins (56), more evident in our system for VP-2, and although blots did not resolve these protein forms as did the gels described below, good immunoreactivity of VP-1 and of all VP-2 subspecies for our capsid antiserum was apparent. The pIs of these proteins were approximately 8.2 to 8.4 and 6.8 to 7.2, respectively, in

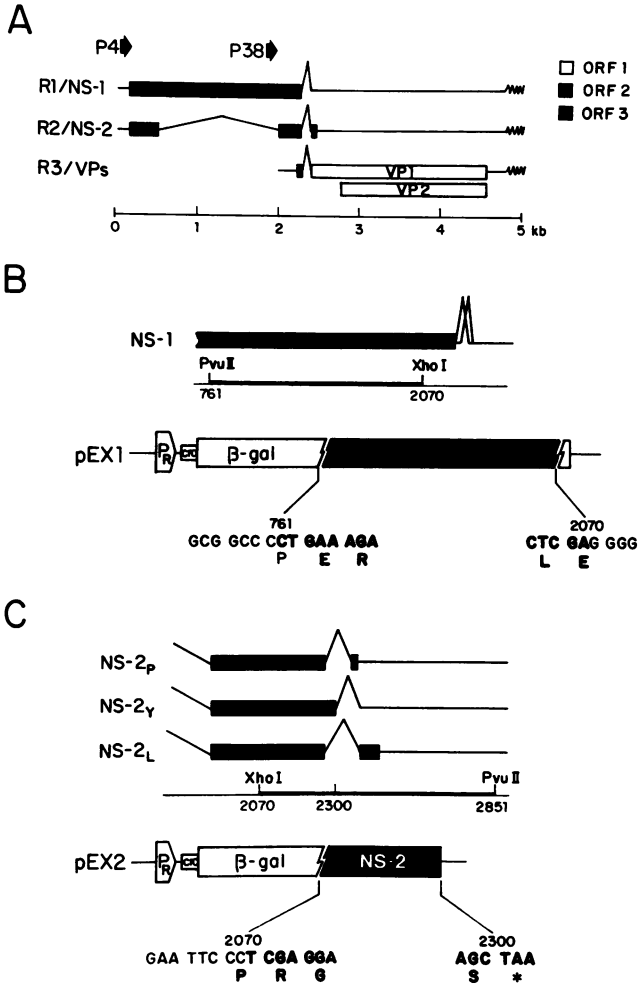

FIG. 1. Plasmid constructs to express NS fusion proteins of the parvovirus MVMp. (A) Organization of the MVM genome. The coding regions of the virus genome are boxed in their respective messengers. Thick arrows indicate the positions of the viral promoters. ORF, open reading frame. (B) Cloning strategy to express the NS-1 protein. A *Pvu*II-*Xho*I NS-1-specific coding region was inserted in frame at the C terminus of the β-Gal gene of plasmid pEX-1. Restriction sites selected for the construct and sequences at the cloning sites are outlined. (C) Expression construct for the NS-2 protein. The alternatively spliced NS-2 protein isoforms are represented. An *Xho*I-*Pvu*II restriction fragment expanding this region was cloned at the *Sma*I site of plasmid pEX-2 in the coding frame of the NS-2 second exon. Amino acids at the fusion points and the NS-2 stop codon are indicated.

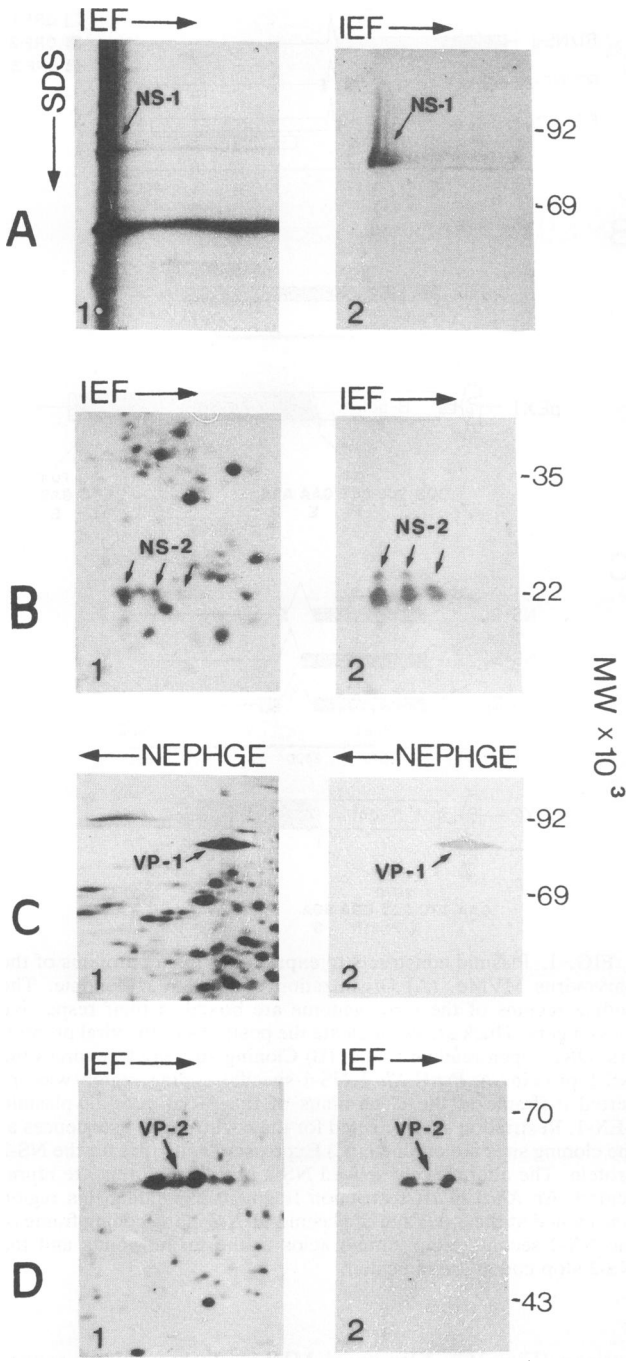

FIG. 2. Immune identification of MVMp proteins by blot analysis of 2-D gels. Total cellular extracts from A9 cells infected by MVMp and labeled at 12 to 16 hpi with [^{35}S]methionine were resolved by 2-D gel electrophoresis (IEF and NEPHGE) and electroblotted to nitrocellulose membranes as explained in Materials and Methods. The filters were exposed in autoradiography to localize the labeled proteins (1) and subsequently probed with the indicated monospecific polyclonal antisera (2). (A) β-Gal–NS-1 antiserum; (B) β-Gal–NS-2 antiserum; (C and D) capsid antiserum. Only the areas of the filters with immunoreactive spots are shown. MW, molecular weight.

agreement with reported values (56). The importance of the N-terminal basic region of VP-1 in determining this pI switch has previously been noticed (16). As expected, the third MVM structural protein, VP-3, which appears late in the infection (77), was not found to be induced on these gels in the 16-hpi samples, and its modification pattern in purified virions is described below.

MVMp-induced protein species and phosphorylation stages at high resolution. We combined a 2-D electrophoresis system with ^{35}S labeling to high specific activity in an attempt to increase the resolution of the protein species induced by the MVMp virus in a productive infection and quantitate the average abundance of each species in the population of permissive A9 cells. Samples of growing A9 cells infected by MVMp and labeled at 12 to 16 hpi with 1 mCi of [^{35}S]methionine per ml were submitted to 2-D gel electrophoresis at the conditions for high resolution described in Materials and Methods. The virus-induced proteins identified by their specific immunoreactivity were quite evident in these gels (Fig. 3B) in comparison with those of uninfected cells (Fig. 3A). The high level of induction makes the MVMp-coded polypeptides among the most abundant proteins of the infected cells, even in an asynchronized population. The NS-1 protein was resolved in the form of a continuous spot expanded between pI values of 7.2 to 7.8, a basic character that must be determined by the net negative charge at both amino and carboxy termini of this protein (39). The NS-2 isoforms were resolved as three pair of spots at a pI value of approximately 5.5. Quantitation by scanning laser densitometry indicated that the isoform to the left was twice as abundant as the one to the right and as much as seven times more abundant than the central pair of spots. These numbers are in rough agreement with the relative quantities of the three NS-2 isoforms estimated by immunoprecipitation with specific antipeptide antibodies (18) and gives the order P-L-Y (from left to right) in the IEF gels. The larger structural protein VP-1 was focused as a thick spot with some microheterogeneity that could correspond to several species gathered by the lower resolving power in this region of the NEPHGE gels. In contrast, the VP-2 protein that focused in the neutral region of the IEF gels could be resolved in the form of at least six isoelectric species or subtypes. A more comprehensive description of the VP-2 subtypes is provided below.

The effect that modifications by phosphate radicals might have on these protein forms was investigated by a similar study at high 2-D resolution performed with infected cells labeled at 12 to 16 hpi with 1 mCi of [^{32}P]phosphate per ml (Fig. 4). All MVMp proteins showed phosphorylated species, but the degree of phosphorylation varied dramatically. The capsid proteins were barely detectable in these gels, although VP-2 subtypes were clearly induced as phosphoproteins (Fig. 4C). The NS-1 protein was also poorly phosphorylated, as judged by the faint induced label in the migration region of this protein. However, these 2-D gels showed a prominent and highly heterogeneous phosphorylated component at neutral pI with a molecular weight close to that of NS-1 (marked by a thick arrow in Fig. 4C) that was not detected in the ^{35}S-labeled protein gels (Fig. 3B). This component could correspond to a minor hyperphosphorylated form described for the NS-1 protein in polyacrylamide gel electrophoresis (PAGE) (52) that would not be immunoreactive for our monospecific antiserum raised against an unmodified bacterially expressed β-Gal–NS-1 fusion protein. On the other hand, all three NS-2 isoforms were phosphorylated; each appeared to be composed of two species, the

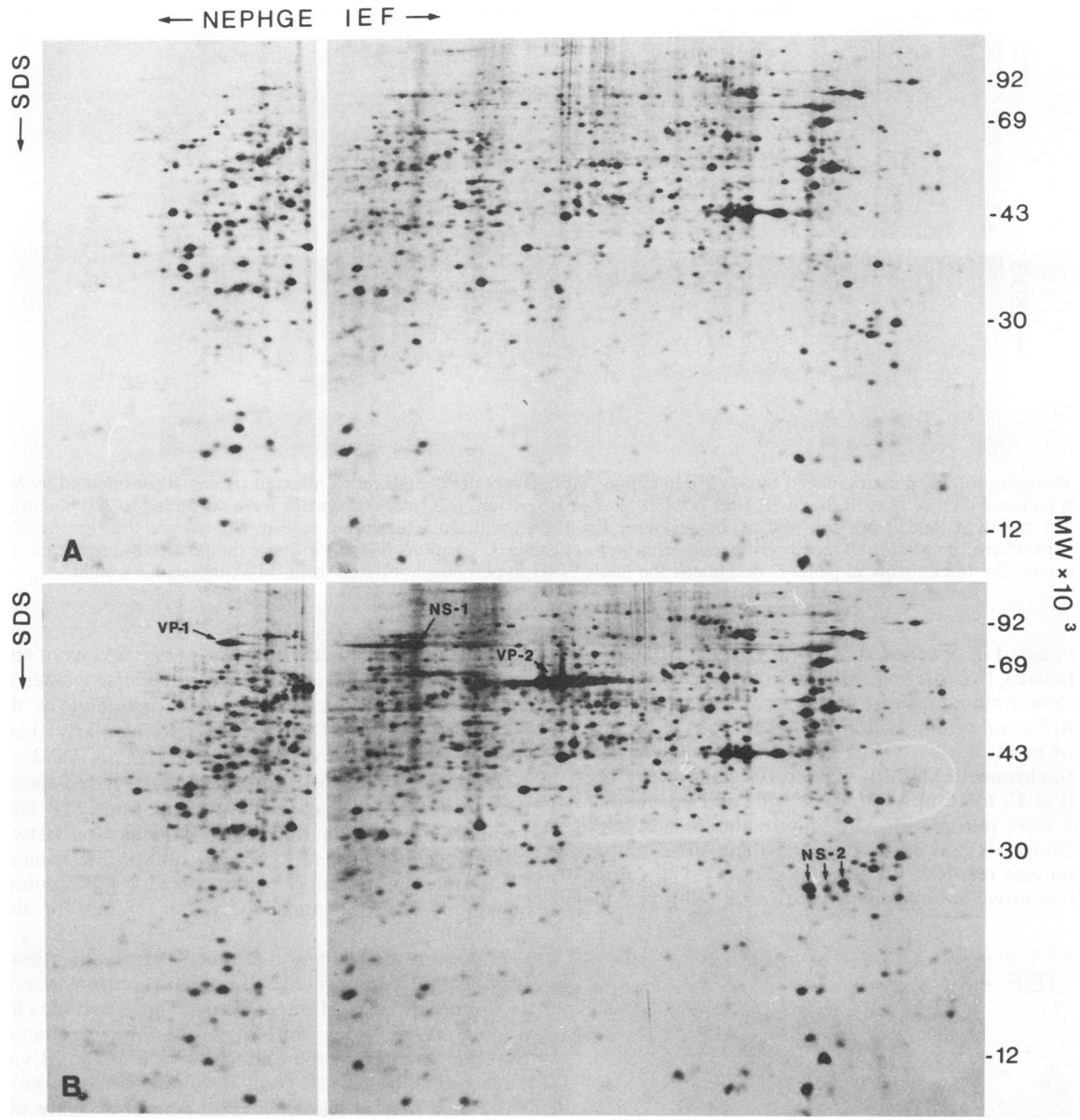

FIG. 3. 2-D map of the MVMp-induced protein species in A9 mouse fibroblasts. Autoradiograms of 2-D gels (IEF and NEPHGE) of [^{35}S]methionine-labeled polypeptides from mock-infected (A) and MVMp-infected (B) A9 cells pulse-labeled at 12 to 16 hpi. Gels were processed for fluorography and exposed for 48 h. In IEF, the pH ranged from 7.8 (left) to 4.4 (right); NEPHGE, the pH ranged from 7.8 (right) to 9.0 (left). Arrows indicate the positions in the gel of the MVMp polypeptides as deduced from the immune recognition criteria. MW, molecular weight.

upper one being slightly more labeled, although other minor components were also seen (Fig. 4D). Notably, the lowest-abundance NS-2_L isoform (Fig. 3B) (18) was the most heavily phosphorylated (Fig. 4D); in fact, this form becomes a major component in the global pattern of phosphoproteins present in MVMp-infected A9 cells.

Regulation of VP-2 subspecies by the capsid assembly and genome encapsidation processes. We have studied the importance of structural protein modifications in MVMp morphogenesis by determining the changes that take place on the VP-2 subtype composition, as it is the best-resolved protein in our gel system and the major component of the capsid. First, to study whether the VP-2 modifications are imposed by capsid assembly, infected cells were labeled at 14 hpi by a 5-min pulse with [^{35}S]methionine, and the total cell lysate was analyzed by IEF gels. As shown in Fig. 5A, the six VP-2 subspecies were synthesized after the short pulse-label at the ratio found in a continuous 12- to 16-hpi labeling period (Fig. 3B), and this modification could not be chased into a pattern distinct from the pulse profile (Fig. 5B). Thus, VP-2 is modified by cotranslational or immediately posttranslational mechanisms, apparently through unconnected biosynthetic pathways, in a way temporaneously unrelated to the ongoing virus assembly. As indicated in Fig. 5A, the VP-2 subspecies

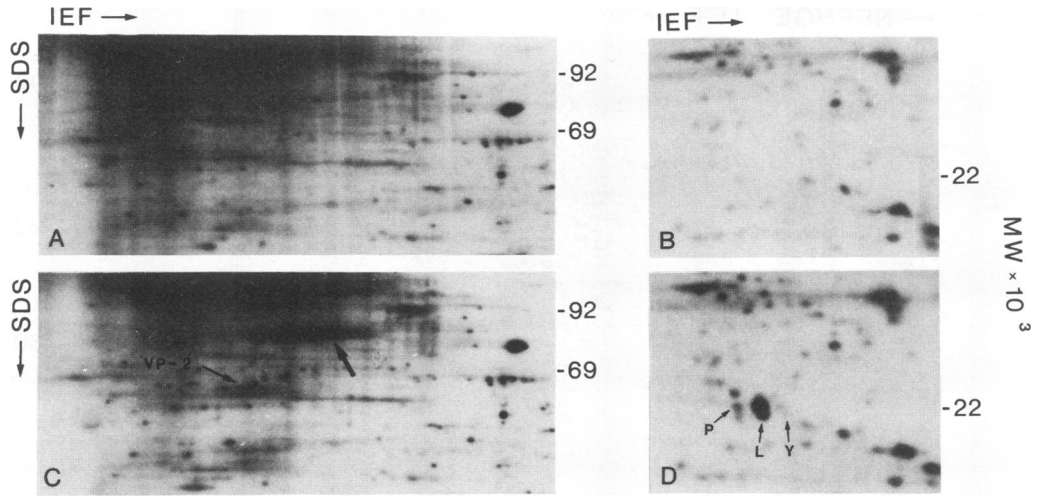

FIG. 4. Phosphoprotein species induced by MVMp infection. Monolayers of A9 cells mock infected (A and B) or infected by MVMp (C and D) were pulse-labeled at 12 to 16 hpi with 1 mCi of [^{32}P]phosphate per ml, and total cell lysates were subjected to 2-D electrophoresis. A total of 10^6 cpm was loaded per gel, and exposures were for 3 days with an intensifying screen. Shown are the regions of the IEF autoradiograms where the MVMp-induced phosphoproteins were evidenced. Positions of the VP-2 and the three NS-2 isoforms (P, L, and Y) are indicated. The thick arrow in panel C designates the likely NS-1 hyperphosphorylated form. MW, molecular weight.

have been named in order of increasingly acidic pI as three abundant (a to c), two intermediate-abundance (d and e), and one much lower abundance (f) species.

The contribution of the distinct VP-2 subtypes to the final structure of newly formed virus and capsids was analyzed next. Unsynchronized MVMp-infected A9 cells were ^{35}S or ^{32}P labeled at 12 to 16 hpi, empty capsids and intracellular full virions were purified by consecutive equilibrium gradients (see Materials and Methods), and their VP-2 subtype composition was resolved on 2-D gels (Fig. 6). The composition and relative abundance of the VP-2 subtypes that formed the purified empty capsids (Fig. 6A) were analogous to the pattern of induction found in cellular lysates (Fig. 3B and 5); in fact, both films could be matched for the VP-2 spots. When ^{32}P-labeled capsids were similarly analyzed, a uniform distribution of the label across the VP-2 subtypes was observed (Fig. 6B). Since phosphorylated species with decreasing pI are expected to show more ^{32}P label, this result is most likely due to a compensation between the abundance of each subtype and its specific radioactivity. Consequently, assembly of the capsid is not regulated by a specific prominent phosphorylation of any of the VP-2 subtypes.

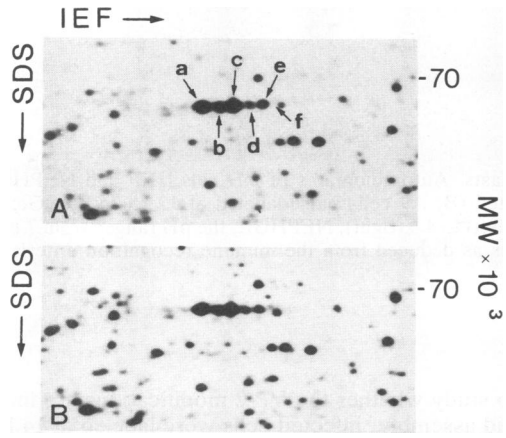

FIG. 5. Pulse-chase labeling of VP-2 subspecies. A9 cells were infected by MVMp; at 12 hpi, cells were incubated for 2 h with methionine-free medium supplemented with 5% dialyzed FCS and pulse-labeled (14 hpi) for 5 min with 1 mCi of [^{35}S]methionine per ml in the same medium. At the completion of labeling, cells were harvested either immediately (A) or after the label was chased by 2 h of culture in DMEM–10% FCS containing excess methionine (B). Samples were subjected to IEF electrophoresis at the conditions indicated in Materials and Methods for high-resolution analysis. The six VP-2 subtypes are named in order of increasingly acidic pI. MW, molecular weight.

However, a strikingly different VP-2 modification pattern was observed in purified full immature virions harvested at 16 hpi before lysis of the cultures. These particles harbored a more complex repertoire of VP-2 subtypes, characterized by a lengthening of the pattern toward acidic pI values. A virus preparation with good resolution of the whole set of VP-2 subtypes is shown in Fig. 6C. The highly abundant group is now composed of subtypes a to e, g, i, and k, while subtypes with intermediate abundance are f, h, and k, and l is a low-abundance subtype. Thus, a rearrangement in the VP-2 composition is imposed by the viral genome encapsidation, and six subtypes (g to l) present in full virions were not seen in empty capsids. The evidence that additional acidic subtypes accompany genome encapsidation was strengthened by the finding that ^{32}P-labeled full virions (Fig. 6D) showed a significant fraction of the label at pI values more acidic than the focusing position of the empty capsid, but the lower 2-D resolution of ^{32}P-labeled samples made it impossible to establish the contribution of each of the newly formed phosphorylated subtypes to this pattern.

Many of these features are shared by the larger VP-1 protein. This structural protein was also assembled under a certain degree of modification and remained phosphorylated in empty and full particles (not shown). The lower resolution power of the NEPHGE system did not allow a clear demonstration of the changes, if any, in the number of VP-1 subtypes in these studies.

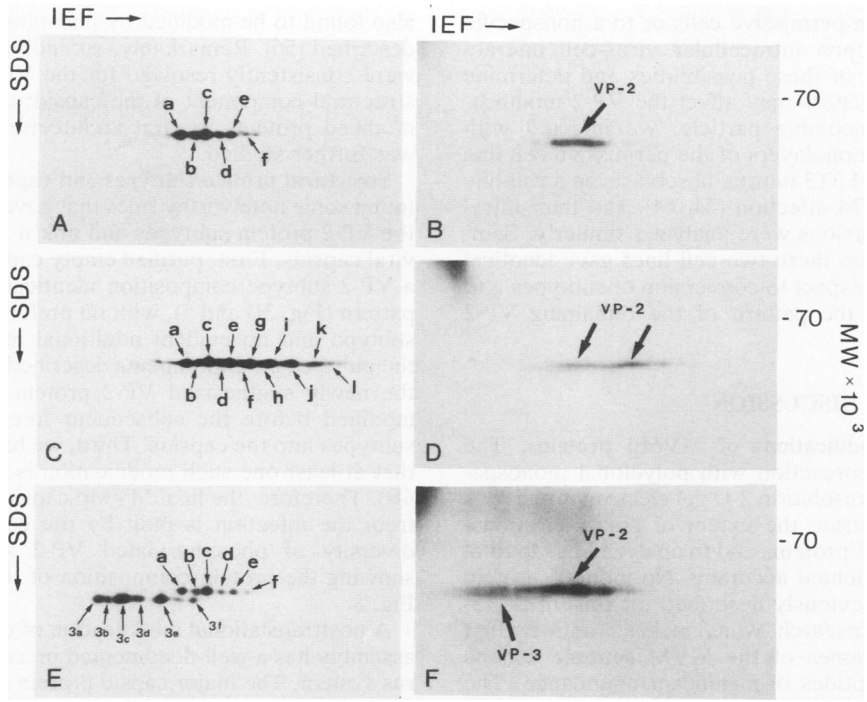

FIG. 6. 2-D analysis of the VP-2 and VP-3 subtypes in purified MVMp particles. Autoradiographs of IEF gels show the ^{35}S- and ^{32}P-labeled VP-2 and VP-3 protein forms in purified empty capsids (A and B) and full immature (C and D) and mature (E and F) virions. An average of 5×10^4 ^{35}S cpm or 2×10^5 ^{32}P cpm was loaded per sample; the gels were processed as described in Materials and Methods and exposed for 4 to 10 days at −80°C. ^{35}S-labeled protein subtypes are designated in order of increasingly acidic pI. MW, molecular weight.

Proteolytic processing of VP-2 subtypes during maturation and virus entry. The structural VP-3 protein results from the cleavage of VP-2 once the viral DNA is packaged (77) and has a pI close to neutral (56). Consequently, we sought VP-3 in samples of mature virions to determine its degree of microheterogeneity and to explore whether any of the VP-2 subtypes act preferentially as precursors for VP-3 in the proteolytic reaction. Virions were purified at 60 hpi from supernatants of lysed cultures labeled with [^{35}S]methionine or [^{32}P]phosphate as described in Materials and Methods and then subjected to IEF gel analysis. VP-3 appeared in the form of five to seven subtypes at a pI slightly more basic than those of most VP-2 subtypes (Fig. 6E) and was phosphorylated more weakly (Fig. 6F). VP-2 subtypes were also phosphorylated in mature virions, but it is noteworthy that we observed a shortening of the VP-2 modification to a pattern indistinguishable in subtype composition and relative abundance from that seen in empty capsids (Fig. 6A) and total induced proteins (Fig. 3B and 5). Thus, mature virions lack the VP-2 subtypes g to l found in full immature virions.

VP-2 conversion to VP-3 was reported to increase in samples of internalized virions in a time-dependent manner, with a linear kinetic up to 6 hpi (50). Therefore, we explored the precursor-product relationship between VP-2 subtypes and VP-3 by studying the appearance of VP-3 in the infection process and its relationship to any alteration in the VP-2 pattern. Purified ^{35}S-labeled immature virus harboring all VP-2 subtypes and lacking VP-3 (Fig. 7A) was used to infect A9 cells, and 6-hpi internalized viral proteins were analyzed. IEF gels of these samples (Fig. 7B) revealed that VP-3 appearance in internalized virions also correlates with the lack of VP-2 subtypes g to l. This VP-2 subtype-to-VP-3 conversion could correspond to a mechanism required for

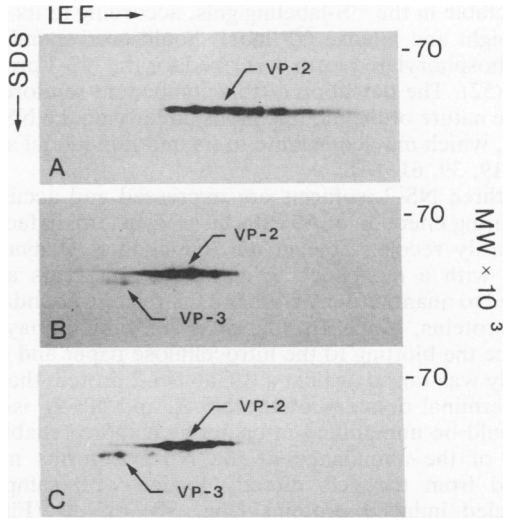

FIG. 7. Conversion of VP-2 species to VP-3 in internalized full virions. Monolayers of 2×10^6 cells grown in 60-mm-diameter dishes were washed with PBS and inoculated with 4×10^4 cpm of purified ^{35}S-labeled full immature virions in 0.5 ml of PBS–0.1% FCS. After 1 h of adsorption at 37°C, the inoculum was removed, the cells were washed three times with PBS, medium with 10% FCS was added, and the infection was allowed to proceed for 6 h at 37°C. Cells were finally washed twice again with PBS and scraped in 2-D lysis buffer. Shown are IEF gels of VP-2 and VP-3 virus proteins in the inoculum (A) and internalized for 6 h in A9 cells (B) or NIH 3T3 fibroblasts (C). The same result was obtained in infections of NB324K cells (not shown). Exposures were for 3 days at −80°C. MW, molecular weight.

the infection process in permissive cells or to a nonspecific proteolytic cleavage upon intracellular virus-cell interactions. To rule out any of these possibilities and determine whether cell permissiveness may affect the VP-2 modification pattern of the incoming particle, we infected with labeled purified virus monolayers of the permissive cell line NB324K (76) or of NIH 3T3 murine fibroblasts as a cell line nonpermissive for MVM infection (44, 64), and their intracellular subtype conversions were analyzed similarly. Samples obtained 6 hpi from these two cell lines gave identical results (Fig. 7C) with respect to conversion of subtypes g to l to VP-3 as well as the pattern of the remaining VP-2 subtypes.

DISCUSSION

Posttranslational modifications of MVMp proteins. The combination of immunoreaction with polyclonal monospecific antisera and high-resolution 2-D gel electrophoresis has allowed us to demonstrate the extent of posttranslational modifications of the NS proteins and to analyze MVMp total proteins with unprecedented accuracy. No induced protein other than the ones previously described for this virus (15, 16) was identified in our search, which makes it unlikely that other open reading frames of the MVM genome can be translated into polypeptides of significant abundance. The extensive use of posttranslational modifications by MVMp proteins is best illustrated for NS-1. NS-1 was found in the gels in the form of two components represented by widely spread spots. The major one was a basic, highly heterogeneous but poorly phosphorylated component, which suggests that one or more other kinds of substituents must account for this electrofocusing behavior. The second one we consider a neutral heterogeneous spot that although undetectable in the ^{35}S-labeling gels, according to its molecular weight and intense ^{32}P label should correspond to the hyperphosphorylated form described for the NS-1 protein in PAGE (52). The detection of this component reinforces the multiple nature of the modifications underlying the NS-1 2-D pattern, which may contribute to its multifunctional activity (9, 17, 19, 39, 61, 84).

The three NS-2 isoforms are expressed and accumulate early during infection of A9 cells by MVMp (18); in fact, they were easily recognizable in the immunoblot analysis performed with a monospecific antibody. Our blots are not designed to quantitatively compare the relative abundance of these proteins, since (i) the phosphorylation may itself influence the blotting to the nitrocellulose paper and (ii) our antibody was raised against a β-Gal–NS-2 protein that lacks the C-terminal domains of the NS-2$_P$ and NS-2$_L$ isoforms and would be unmodified in bacteria. A more reliable estimation of the abundance of the NS-2 isoforms may be deduced from the gels directly loaded with samples of ^{35}S-labeled induced proteins (Fig. 3B) or ^{32}P (Fig. 4D) pulse-labeled at 12 to 16 hpi. When these autoradiograms are quantitatively compared, the least abundant NS-2$_L$ isoform was found to be the most highly phosphorylated one within this large interval of labeling of an asynchronous cell population. Thus, there is every reason to believe that the unique C-terminal exon of this isoform must either be a site of preferential phosphorylation or determine a peculiar subcellular traffic of this protein where phosphorylation in other domains may take place. It remains to be studied whether these phosphorylations play any role in the functions ascribed to the NS-2 proteins (40, 45, 46).

The three structural proteins VP-1, VP-2, and VP-3 were also found to be modified by phosphorylation as previously described (56). Remarkably, six individual isoelectric forms were consistently resolved for the VP-2 protein, the major structural component of the capsid; thus, the role of these modified proteins in viral architecture and morphogenesis was further studied.

Structural protein subtypes and capsid assembly. We have found some noteworthy rules that govern the biosynthesis of the VP-2 protein subtypes and link it to their assembly into viral capsids. First, purified empty capsids (Fig. 6A) showed a VP-2 subtype composition identical to the induced VP-2 pattern (Fig. 3B and 5), with no preferential selection of any subtype and no evident additional modifications. Second, the pulse-chase experiments described in Fig. 5 indicate that the newly synthesized VP-2 protein is posttranslationally modified before the subsequent free assembly of the six subtypes into the capsids. Third, we have also demonstrated that at least one such modification is phosphorylation (Fig. 6B). Therefore, the final MVMp capsid structure that results from the infection is built by the coordination of a fixed diversity of phosphorylated VP-2 subtypes. A drawing showing the protein composition of the capsid is shown in Fig. 8.

A posttranslational modification of capsid subunits before assembly has a well-documented precedent in the papovavirus system. The major capsid protein (VP-1) of simian virus 40 and of mouse and other nonmammalian polyomaviruses is also differentially modified after translation by phosphorylation (31, 48, 58) at Ser and Thr residues (1, 24) and by other modifications that are believed to contribute to the at least six isoelectric forms of the protein (7, 24). The significance of VP-1 phosphorylation in papovavirus assembly remains controversial. Self-assembly into polymorphic aggregates and capsid-like structures was demonstrated with unmodified VP-1 expressed in *E. coli* (65). Nevertheless, mutants of polyomavirus that are deficient in the phosphorylated VP-1 species were blocked in assembly (24, 25). Thus, it may be hypothesized that VP-1 modifications are required for efficient and accurate assembly, namely, promoting the switch of capsomere bonding specificity and the bundling of VP-1 molecules in three groups of interactions among pentameres, before being clamped by the flexible C-terminal tentacle in the all-pentamere T=7 polyomavirus capsid structure (41).

Interestingly, the major VP-2 protein of MVMp is also modified to six subtypes before their assembly into a simpler capsid that is formed by an estimated 60 molecules of VP-1 and VP-2 in an approximate ratio of 1:5 (16). Although differentially phosphorylated species do not seem to be needed for the T=1 parvovirus icosahedron (80), it is tempting to speculate that if the VP-1 monomeres are asymmetrically packaged or clustered in two capsomeres (51), the surrounding VP-2 subunits exposed to such a nonequivalent chemical environment (33) may require differential modifications to form a highly ordered symmetrical framework.

Changes in VP-2 subtypes associated with DNA encapsidation and virus maturation. Phosphorylations of the capsid proteins in several virus systems have been reported to be required for the DNA-coat interaction and the assembly into virions (29; reviewed in reference 38). In MVMp, these modifications accompany genome encapsidation and, if a precursor-product relationship between capsid and full virions is assumed, takes place on a capsid already composed of modified monomeres. The result is that, as shown in the model represented in fig. 8, up to 12 VP-2 subtypes can be resolved by 2-D analysis of full immature particles. However, we have found some variability in the number of VP-2

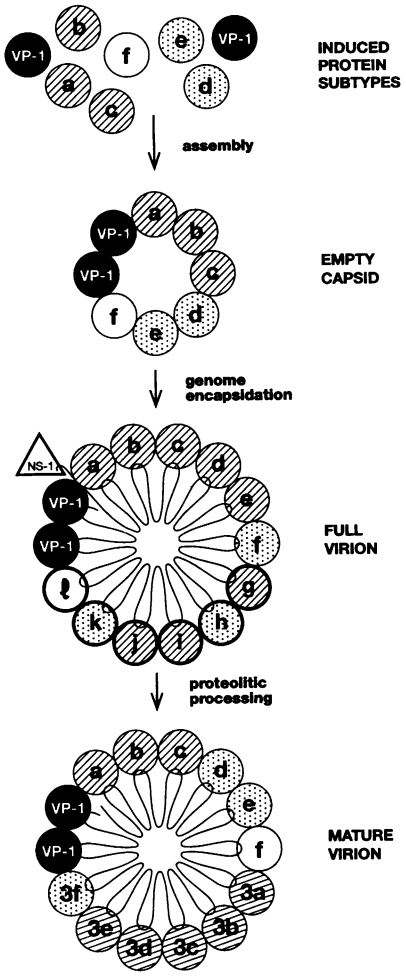

FIG. 8. MVMp protein forms in morphogenetic coat transitions. VP proteins are represented by spheres alphabetically named in order of increasingly acidic pI. Those corresponding to the VP-2 and VP-3 subtypes are drawn in three categories according to their relative abundance as estimated by [^{35}S]methionine labeling: low (open circles) medium (dotted circles), and high (striped circles). The thickly outlined VP-2 species in the immature full virion represent transiently modified subtypes more sensitive to the proteolytic cleavage that yields VP-3 subtypes (3a to 3f). The rosette is an arbitrary array of the viral ssDNA to accommodate the described 11% regular interaction with each capsid subunit (80). VP-1 subunits are represented clustered in the capsid, as suggested by cross-linking experiments (51). The covalent linkage between the 5' end of the genome and an NS-1 molecule placed outside the virus particle (17) and a noncovalent binding of the 3' hairpin with VP-1 molecules (83) are also illustrated. A rationale for the model is provided in the text.

subtypes among preparations of these particles that might be caused by occasional overlapping of protein forms in the gels or, more likely, by the fact that several stages of capsid phosphorylation are compatible with the viral DNA encapsidation. Because, as explained below, these more acidic VP-2 protein forms are precursors of VP-3, this heterogeneity would explain the variable VP-2-to-VP-3 ratio normally found in MVMp preparations (23, 50, 77).

The posttranslational modifications in the coat subunits accompanying the ongoing DNA packaging process raise two important issues regarding MVM morphogenesis that are beyond the scope of this report. First, how do DNA and capsid subunit conformations coordinately switch to arrange an icosahedrally ordered viral genome into the protein shell (80)? The transient modification of VP subtypes that occurs coordinately with genome encapsidation may catalyze a pleomorphic stage of the capsid, allowing the allocation of the viral genome. Second, the involvement of phosphate radicals in the course of the encapsidation may imply the association of a kinase activity with the packaging complex. Given that in the autonomous parvoviruses, ssDNA synthesis is concomitant with packaging (62), this machinery includes the NS-1 protein bound to the 5' viral DNA end (17), a protein with an ATPase activity (84) that could cooperate in the reaction.

Packaged VP-1 and VP-2 proteins differ in sensitivity to proteases such as trypsin or chymotrypsin (53, 78). Virion VP-2 but not capsid VP-2 may be cleaved proteolytically to VP-3, mimicking the process that takes place during virus maturation (77). Therefore, conformational or chemical modifications should occur specifically in the VP-2 protein of full virions (16), making its N-terminal domain more accessible to proteolytic maturation cleavage. We have demonstrated posttranslational modifications in VP-2 that fulfill these criteria: subtypes g to l were exclusively seen in the VP-2 of immature full virions (Fig. 6C) and were specifically removed during virus maturation (Fig. 6E) or reinfection (Fig. 7) as the VP-3 subtypes appeared in the gels. These data support the model outlined in Fig. 8, in which acidic VP-2 subtypes g to l convert to VP-3 by preferential proteolytic cleavage of the more phosphorylated polypeptides. Accumulation of phosphate residues at the VP-2 N terminus may be responsible for the outward projection of this domain observed in the three-dimensional structure of the canine parvovirus full virion (80). This, in turn, would make it more sensitive to proteolysis, both by an increased accessibility to proteases and by the positive modulation that substrate phosphorylation may exert on chymotrypsin cleavage activity (63). The coincidence in the number of VP-2 and VP-3 subtypes suggests that all six VP-2 isoelectric forms act as precursors of VP-3 through the phosphorylation-cleavage process.

Protein modifications in MVMp infection. Among the MVM proteins, VP-2 is the major component of the MVM capsid and is thought to contain catalytic activities of paramount importance for the virus life cycle, including encapsidation of the virus progeny genome (81) and interaction of the incoming particle with the cells (2, 5). A productive infectious pathway could be linked to specific VP modifications of the internalized virions on their way to the cell nucleus. When purified labeled virus harboring all of VP-2 subtypes a to l was used to infect cells differing in the degree of permissiveness to MVMp infection, the bulk of internalized virions analyzed at 6 hpi underwent in all cases a sharp reduction in the number of subtypes (Fig. 7), to a pattern similar to the one observed in empty capsids or mature virions (Fig. 6) and accompanied by the yield of an equal number of VP-3 subtypes. Therefore, neither proteolytic processing itself nor subtypes composition explains the commitment of the internalized virions with a productive infectious pathway. Further experiments are required to determine whether any selective protein modification takes place in the small proportion of infectious virions present in the inoculum (50) or whether the precise subcellular compartment where these modifications occur differs in cells with variable levels of permissiveness.

From the standpoint of posttranslational modifications,

the MVMp virion is a complex macromolecular entity, composed of 60 copies of phosphorylated structural protein forms: some VP-1, up to 12 VP-2 subtypes (in the immature particles), and 5 to 7 VP-3 subtypes (only in mature virions). Such a highly modified protein coat may be common in parvoviruses, as several proteins of the autonomous porcine parvovirus were also reported to be phosphorylated (42). Moreover, distinct functions have been assigned to the VP-1 phosphorylated species of the polyomavirus capsid, such as host cell-receptor interaction (7) or encapsidation into infectious virus (24–26). Likewise, different roles may apply for the individual VP subtypes in the MVMp life cycle besides those discussed in this report, constituting additional means to maximize the genetic information of these genetically simple viruses. It would be interesting to establish the extent to which each of these components contributes to the intracellular interactions and morphogenetic processes that make certain differentiated or transformed cells permissive to virus infection (44, 75). This knowledge would ultimately allow researchers to gain an overall understanding of parvovirus pathogenicity at the organism level.

ACKNOWLEDGMENTS

We are very grateful to Peter Tattersall and Thomas L. Benjamin for thoughtful critical discussions regarding the manuscript, to I. Ormán for excellent technical assistance, and to J. C. Segovia and J. M. Gallego for help in cell labelings. The computer graphic design by SUCALA is also acknowledged.

This work was supported by grants BIO 88-C666-C02-01 and SAF 92-1014-C02-01 from the Comisión Interministerial de Ciencia y Tecnología and by an institutional grant from Fundación Ramón Areces to the Centro de Biología Molecular "Severo Ochoa." J.C.R. was the recipient of a predoctoral fellowship (FPI) from the Spanish Ministry of Education.

REFERENCES

1. **Anders, D. G., and R. A. Consigli.** 1983. Comparison of nonphosphorylated and phosphorylated species of polyomavirus major capsid protein VP1 and identification of the major phosphorylation region. J. Virol. **48**:206–217.
2. **Antonietti, J.-P., R. Sahli, P. Beard, and B. Hirt.** 1988. Characterization of the cell type-specific determinant in the genome of minute virus of mice. J. Virol. **62**:552–557.
3. **Astell, C. R., E. M. Gardiner, and P. Tattersall.** 1986. DNA sequence of the lymphotropic variant of minute virus of mice, MVM(i), and comparison with the DNA sequence of the fibrotropic prototype strain. J. Virol. **57**:656–669.
4. **Astell, C. R., M. Smith, M. B. Chow, and D. C. Ward.** 1979. Structure of the 3'-hairpin termini of four rodent parvovirus genomes: nucleotide sequence homology at origins of DNA replication. Cell **17**:691–703.
5. **Ball-Goodrich, L. J., R. D. Moir, and P. Tattersall.** 1991. Parvoviral target cell specificity: acquisition of fibrotropism by a mutant of the lymphotropic strain of minute virus of mice involves multiple amino acid substitutions within the capsid. Virology **184**:175–186.
6. **Ball-Goodrich, L. J., and P. Tattersall.** 1992. Two amino acid substitutions within the capsid are coordinately required for acquisition of fibrotropism by the lymphotropic strain of minute virus of mice. J. Virol. **66**:3415–3423.
7. **Bolen, J. B., D. G. Anders, J. Trempy, and R. A. Consigli.** 1981. Differences in the subpopulations of the structural proteins of polyoma virions and capsids: biological functions of the multiple VP-1 species. J. Virol. **37**:80–91.
8. **Brown, D. D., and L. A. Salzman.** 1984. Sequence homology between the structural proteins of Kilham rat virus. J. Virol. **49**:1018–1020.
9. **Caillet-Fauquet, P., M. Perros, A. Brandenburger, P. Spegelaere, and J. Rommelaere.** 1990. Programmed killing of human cells by means of an inducible clone of parvoviral genes encoding non-structural proteins. EMBO J. **9**:2989–2995.
10. **Clemens, K. E., D. R. Cerutis, L. R. Bueger, C. Q. Yang, and D. J. Pintel.** 1990. Cloning of minute virus of mice cDNA and preliminary analysis of individual proteins expressed in murine cells. J. Virol. **64**:3967–3973.
11. **Cornelis, J. J., P. Becquart, N. Duponchel, N. Salome, B. L. Avalosse, M. Namba, and J. Rommelaere.** 1988. Transformation of human fibroblasts by ionizing radiation, a chemical carcinogen, or simian virus 40 correlates with an increase in susceptibility to the autonomous parvovirus H-1 and minute virus of mice. J. Virol. **62**:1679–1686.
12. **Cornelis, J. J., Y. Q. Chen, N. Spruyt, N. Duponchel, S. F. Cotmore, P. Tattersall, and J. Rommelaere.** 1990. Susceptibility of human cells to killing by the parvovirus H-1 and minute virus of mice correlates with viral transcription. J. Virol. **64**:2537–2544.
13. **Cotmore, S. F., L. J. Sturzenbecker, and P. Tattersall.** 1983. The autonomous parvovirus MVM encodes two nonstructural proteins in addition to its capsid polypeptides. Virology **129**:333–343.
14. **Cotmore, S. F., and P. Tattersall.** 1986. The NS-1 polypeptide of the autonomous parvovirus MVM is a nuclear phosphoprotein. Virus Res. **4**:243–250.
15. **Cotmore, S. F., and P. Tattersall.** 1986. Organization of nonstructural genes of the autonomous parvovirus minute virus of mice. J. Virol. **58**:724–732.
16. **Cotmore, S. F., and P. Tattersall.** 1987. The autonomously replicating parvoviruses of vertebrates. Adv. Virus Res. **33**:91–173.
17. **Cotmore, S. F., and P. Tattersall.** 1989. A genome-linked copy of the NS-1 polypeptide is located on the outside of infectious parvovirus particles. J. Virol. **63**:3902–3911.
18. **Cotmore, S. F., and P. Tattersall.** 1990. Alternate splicing in a parvoviral nonstructural gene links a common amino-terminal sequence to downstream domains which confer radically different localization and turnover characteristics. Virology **177**:477–487.
19. **Cotmore, S. F., and P. Tattersall.** 1992. In vivo resolution of circular plasmids containing concatemere junction fragments from minute virus of mice DNA and their subsequent replication as linear molecules. J. Virol. **66**:420–431.
20. **Crawford, L. V.** 1966. A minute virus of mice. Virology **29**:605–612.
21. **Doerig, C., B. Hirt, J. P. Antonietti, and P. Beard.** 1990. Nonstructural protein of parvovirus B19 and minute virus of mice controls transcription. J. Virol. **64**:387–396.
22. **Doerig, C., B. Hirt, B. Beard, and J. P. Antonietti.** 1988. Minute virus of mice non-structural protein NS-1 is necessary and sufficient for trans-activation of the viral P39 promoter. J. Gen. Virol. **69**:2563–2573.
23. **Faust, E. A., K. Brudzynska, and J. Morgan.** 1989. Characterization of novel populations of MVM virions containing covalent DNA-protein complexes. Virology **168**:128–137.
24. **Garcea, R. L., K. Ballmer-Hofer, and T. L. Benjamin.** 1985. Virion assembly defect of polyomavirus hr-t mutants: underphosphorylation of major capsid protein VP-1 before viral DNA encapsidation. J. Virol. **54**:311–316.
25. **Garcea, R. L., and T. L. Benjamin.** 1983. Host range transforming gene of polyoma virus plays a role in virus assembly. Proc. Natl. Acad. Sci. USA **80**:3613–3617.
26. **Garcea, R. L., D. A. Talmarge, A. Harmatz, R. Freund, and T. L. Benjamin.** 1989. Separation of host range from transformation functions of the hr-t gene of polyomavirus. Virology **168**:312–319.
27. **Gardiner, E. M., and P. Tattersall.** 1988. Mapping of the fibrotropic and lymphotropic host range determinants of the parvovirus minute virus of mice. J. Virol. **62**:2605–2613.
28. **Gardiner, E. M., and P. Tattersall.** 1988. Evidence that developmentally regulated control of gene expression by a parvoviral allotropic determinant is particle mediated. J. Virol. **62**:1713–1722.
29. **Ghabrial, S. A., and W. M. Havens.** 1992. The *Helminthosporium victoriae* 190S mycovirus has two forms distinguishable

by capsid protein composition and phosphorylation state. Virology **188**:657–665.
30. **Harlow, E., and D. Lane.** 1988. Antibodies, a laboratory manual. Cold Spring Harbor Laboratory, Cold Spring Harbor, N.Y.
31. **Haynes, J. I., II, and R. A. Consigli.** 1992. Phosphorylation of the budgerigar fledgling disease virus major capsid protein VP1. J. Virol. **66**:4551–4555.
32. **Jongeneel, C. V., R. Sahli, G. K. McMaster, and B. Hirt.** 1986. A precise map of splice junctions in the mRNAs of minute virus of mice, an autonomous parvovirus. J. Virol. **59**:564–573.
33. **Klug, A.** 1983. Architectural design of spherical viruses. Nature (London) **303**:378–379.
34. **Knowles, W. J., and M. L. Bologna.** 1983. Isolation of the chemical domains of human erythrocyte spectrin. Methods Enzymol. **96**:305–313.
35. **Labienec-Pintel, L., and D. Pintel.** 1986. The minute virus of mice P39 transcription unit can encode both capsid proteins. J. Virol. **57**:1163–1167.
36. **Lacal, J. C., E. Santos, V. Notario, M. Barbacid, S. Yamazaki, H.-F. Kung, C. Seamans, S. McAndrew, and R. Crowl.** 1984. Expression of normal and transforming H-ras genes in *Escherichia coli* and purification of their encoded p21 proteins. Proc. Natl. Acad. Sci. USA **81**:5305–5309.
37. **Laskey, R. A., and A. D. Mills.** 1975. Quantitative film detection of ^{3}H and ^{14}C in polyacrylamide gels by fluorography. Eur. J. Biochem. **56**:335–341.
38. **Leader, D. P., and M. Katan.** 1988. Viral aspects of protein phosphorylation. J. Gen. Virol. **69**:1441–1464.
39. **Legendre, D., and J. Rommelaere.** 1992. Terminal regions of the NS-1 protein of the parvovirus minute virus of mice are involved in cytotoxicity and promoter *trans* inhibition. J. Virol. **66**:5705–5713.
40. **Li, X., and S. L. Rhode.** 1991. Nonstructural protein NS-2 of parvovirus H-1 is required for efficient viral protein synthesis and virus production in rat cells *in vivo* and *in vitro*. Virology **184**:117–130.
41. **Liddington, R. C., Y. Yan, J. Moulai, R. Sahli, T. L. Benjamin, and S. C. Harrison.** 1991. Structure of simian virus 40 at 3.8-A resolution. Nature (London) **354**:278–284.
42. **Molitor, T. W., H. S. Joo, and M. S. Collett.** 1985. Identification and characterization of a porcine parvovirus nonstructural polypeptide. J. Virol. **55**:554–559.
43. **Morgan, W. R., and D. C. Ward.** 1986. Three splicing patterns are used to excise the small intron common to all minute virus of mice RNAs. J. Virol. **60**:1170–1174.
44. **Mousset, S., and J. Rommelaere.** 1982. Minute virus of mice inhibits cell transformation by simian virus 40. Nature (London) **300**:537–539.
45. **Naeger, L. K., J. Cater, and D. J. Pintel.** 1990. The small nonstructural protein (NS2) of the parvovirus minute virus of mice is required for efficient DNA replication and infectious virus production in a cell-type-specific manner. J. Virol. **64**: 6166–6175.
46. **Naeger, L. K., N. Salomé, and D. J. Pintel.** 1993. NS2 is required for efficient translation of viral mRNA in minute virus of mice-infected murine cells. J. Virol. **67**:1034–1043.
47. **O'Farrell, P. H.** 1975. High resolution two-dimensional electrophoresis of proteins. J. Biol. Chem. **250**:4007–4021.
48. **O'Farrell, P. Z., and H. M. Goodman.** 1976. Resolution of simian virus 40 proteins in whole cell extracts by two-dimensional electrophoresis: heterogeneity of the major capsid protein. Cell **9**:289–298.
49. **O'Farrell, P. Z., H. M. Goodman, and P. H. O'Farrell.** 1977. High-resolution two-dimensional electrophoresis of basic as well as acidic proteins. Cell **12**:1133–1142.
50. **Paradiso, P. R.** 1981. Infectious process of the parvovirus H-1: correlation of protein content, particle density, and viral infectivity. J. Virol. **39**:800–807.
51. **Paradiso, P. R.** 1983. Analysis of the protein-protein interactions in the parvovirus H-1 capsid. J. Virol. **46**:94–102.
52. **Paradiso, P. R.** 1984. Identification of multiple forms of the noncapsid parvovirus protein NCVP-1 in H-1 parvovirus-infected cells. J. Virol. **52**:82–87.
53. **Paradiso, P. R., K. R. Williams, and R. L. Constantino.** 1984. Mapping of the amino terminus of the H-1 parvovirus major capsid protein. J. Virol. **52**:77–81.
54. **Parrish, C. R.** 1991. Mapping specific functions in the capsid structure of canine parvovirus and feline panleukopenia virus using infectious plasmid clones. Virology **183**:195–205.
55. **Parrish, C. R., and L. E. Carmichael.** 1986. Characterization and recombination mapping of an antigenic and host range mutation of canine parvovirus. Virology **148**:121–132.
56. **Peterson, J. L., R. M. K. Dale, R. Karess, D. Leonard, and D. C. Ward.** Comparison of parvovirus structural proteins: evidence for post-translational modification, p. 431–445. *In* D. C. Ward and P. Tattersall (ed.), Replication of mammalian parvoviruses. Cold Spring Harbor Laboratory, Cold Spring Harbor, N.Y.
57. **Pintel, D., D. Dadachanji, C. R. Astell, and D. C. Ward.** 1983. The genome of minute virus of mice, an autonomous parvovirus, encodes two overlapping transcription units. Nucleic Acids Res. **11**:1019–1038.
58. **Ponder, B. A. J., A. K. Robbins, and L. V. Crawford.** 1977. Phosphorylation of polyoma and SV40 virus proteins. J. Gen. Virol. **37**:75–83.
59. **Rhode, S. L., and B. Klaassen.** 1982. DNA sequence of the 5′-terminus containing the replication origin of parvovirus replicative form DNA. J. Virol. **22**:778–793.
60. **Rhode, S. L., III.** 1985. *trans*-activation of parvovirus P38 promoter by the 76K noncapsid protein. J. Virol. **55**:886–889.
61. **Rhode, S. L., III.** 1989. Both excision and replication of cloned autonomous parvovirus DNA require the NS1 (*rep*) protein. J. Virol. **63**:4249–4256.
62. **Richards, R., P. Linser, and R. W. Armentrout.** 1977. Kinetics of assembly of a parvovirus minute virus of mice, in synchronized rat brain cells. J. Virol. **22**:778–793.
63. **Russell, W. C., A. Wedster, I. R. Leith, and G. D. Kemp.** 1989. Phosphorylation of adenovirus DNA-binding protein. J. Gen. Virol. **70**:3249–3259.
64. **Salomé, N., B. van Hille, N. Duponchel, G. Meneguzzi, F. Cuzin, J. Rommelaere, and J. J. Cornelis.** 1990. Sensitization of transformed rat cells to parvovirus MVMp is restricted to specific oncogenes. Oncogenes **5**:123–130.
65. **Salunke, M., D. L. D. Caspar, and R. L. Garcea.** 1986. Self assembly of purified polyomavirus capsid protein VP1. Cell **46**:895–904.
66. **Sambrook, J., E. F. Fritsch, and T. Maniatis.** 1989. Molecular cloning: a laboratory manual, 2nd ed. Cold Spring Harbor Laboratory, Cold Spring Harbor, N.Y.
67. **Santarén, J. F.** 1990. Towards establishing a protein database of Drosophila. Electrophoresis **11**:254–267.
68. **Segovia, J. C., A. Real, J. A. Bueren, and J. M. Almendral.** 1991. *In vitro* myelosuppressive effects of the parvovirus minute virus of mice (MVMi) on hematopoietic stem and committed progenitor cells. Blood **77**:980–988.
69. **Siegl, G.** 1984. Biology and pathogenicity of autonomous parvoviruses, p. 297–362. *In* K. I. Berns (ed.), The parvoviruses. Plenum Press Inc., New York.
70. **Siegl, G., R. C. Bates, K. I. Berns, B. J. Carter, D. C. Kelly, E. Kurstak, and P. Tattersall.** 1985. Characteristic and taxonomy of parvoviridae. Intervirology **23**:61–73.
71. **Spalholz, B. A., and P. Tattersall.** 1983. Interaction of minute virus of mice with differentiated cells: strain-dependent target cell specificity is mediated by intracellular factors. J. Virol. **46**:937–943.
72. **Spegelaere, P., B. V. Hille, N. Spruyt, S. Faisst, J. J. Cornelis, and J. Rommelaere.** 1991. Initiation of transcription from the minute virus of mice P4 promoter is stimulated in rat cells expressing a c-Ha-*ras* oncogene. J. Virol. **65**:4919–4928.
73. **Stanley, K. K., and J. P. Luzio.** 1984. Construction of a new family of high efficiency expression vectors: identification of cDNA clones coding for human liver proteins. EMBO J. **3**:1429–1434.
74. **Tattersall, P.** 1978. Parvovirus protein structure and virion maturation, p. 53–72. *In* D. C. Ward and P. Tattersall (ed.), Replication of mammalian parvovirus. Cold Spring Harbor Laboratory, Cold Spring Harbor, N.Y.

75. **Tattersall, P.** 1978. Susceptibility to minute virus of mice as a function of host cell differentiation, p. 131–149. *In* D. C. Ward and P. Tattersall (ed.), Replication of mammalian parvovirus. Cold Spring Harbor Laboratory, Cold Spring Harbor, N.Y.
76. **Tattersall, P., and J. Bratton.** 1983. Reciprocal productive and restrictive virus-cell interaction of immunosuppressive and prototype strains of minute virus of mice. J. Virol. **46**:944–955.
77. **Tattersall, P., P. J. Cawte, A. J. Shatkin, and D. C. Ward.** 1976. Three structural polypeptides coded for by minute virus of mice, a parvovirus. J. Virol. **20**:273–289.
78. **Tattersall, P., A. J. Shatkin, and D. C. Ward.** 1977. Sequence homology between the structural polypeptides of minute virus of mice. J. Mol. Biol. **111**:375–394.
79. **Towbin, H., T. Staehelin, and J. Gordon.** 1979. Electrophoretic transfer of proteins from polyacrylamide gels to nitrocellulose sheets: procedure and some applications. Proc. Natl. Acad. Sci. USA **76**:4350–4354.
80. **Tsao, J., M. S. Chapman, M. Agbandje, W. Keller, K. Smith, H. Wu, M. Luo, T. J. Smith, M. G. Rossmann, R. W. Compans, and C. R. Parrish.** 1991. The three-dimensional structure of canine parvovirus and its functional implications. Science **251**:1456–1464.
81. **Tullis, G. E., R. B. Lisa, and D. J. Pintel.** 1993. The minor capsid protein VP1 of the autonomous parvovirus minute virus of mice is dispensable for encapsidation of progeny single-stranded DNA but is required for infectivity. J. Virol. **67**:131–141.
82. **Vasudevacharya, J., and R. W. Compans.** 1992. The NS and capsid genes determine the host range of porcine parvovirus. Virology **187**:515–524.
83. **Willwand, K., and B. Hirt.** 1991. The minute virus of mice capsid specifically recognized the 3' hairpin structure of the viral replicative-form DNA: mapping of the binding site by hydroxyl radical footprinting. J. Virol. **65**:4629–4635.
84. **Wilson, G. M., H. K. Jindal, D. E. Yeung, W. Chen, and C. R. Astell.** 1991. Expression of minute virus of mice major nonstructural protein in insect cells: purification and identification of ATPase and helicase activities. Virology **185**:90–98.